Solid-state chemistry shuffling of alkali ions toward new layered oxide materials

Eunice Mumba Mpanga, Romain Wernert, François Fauth, Emmanuelle Suard, Maxim Avdeev, Bernard Fraisse, Paula Sanz Camacho, Dany Carlier, Oleg Lebedev, Simon Cassidy, et al.

Solid-State Chemistry Shuffling of Alkali Ions toward new Layered Oxide Materials

*Eunice Mumba Mpanga,[a] Romain Wernert,[b] François Fauth,[c] Emmanuelle Suard,[d] Maxim Avdeev,[e,f] Bernard Fraisse,[a] Paula Sanz Camacho,[g] Dany Carlier,[g,h] Oleg Lebedev,[i] Simon J. Cassidy,[b] Gwenaëlle Rousse,[h,j,k] Romain Berthelot[a,h]**

[a] ICGM, Univ Montpellier, CNRS, ENSCM, 34095 Montpellier, France

[b] Department of Chemistry, University of Oxford, Inorganic Chemistry Laboratory, Oxford OX1 3QR, U.K.

[c] CELLS−ALBA Synchrotron, Barcelona, 08290, Spain

[d] Institut Laue-Langevin, BP 156, 71 Avenue des Martyrs, 38042 Grenoble, France

[e] Australian Nuclear Science and Technology Organisation, Kirrawee DC, NSW 2232, Australia

[f] School of Chemistry, The University of Sydney, Sydney, NSW 2006, Australia

[g] Bordeaux INP, ICMCB UMR5026, Université Bordeaux, CNRS, Pessac F-33600, France

[h] Réseau sur le Stockage Électrochimique de l'Énergie (RS2E), CNRS, 80039 Amiens, France

[i] CRISMAT, UMR 6508, CNRS-ENSICAEN, Caen 14050, France

[j] Chimie du Solide et Energie, UMR8260, Collège de France, Paris 75231, France

[k] Sorbonne Université, Paris F-75005, France

ORCID numbers
Eunice Mumba Mpanga (0009-0008-3891-0102); Romain Wernert (0000-0002-5073-4008); François Fauth (0000-0001-9465-3106); Emmanuelle Suard (0000-0001-5966-5929); Maxim Avdeev (0000-0003-2366-5809); Bernard Fraisse (0000-0002-4006-5488); Paula Sanz Camacho (0000-0003-4898-8225); Dany Carlier (0000-0002-5086-4363); Oleg Lebedev (0000-0001-

8998-5018); Simon J Cassidy (0000-0002-4297-1425); Gwenaëlle Rousse (0000-0001-8877-0015); Romain Berthelot (0000-0003-1534-2663)

Abstract

Alkali transition metal layered compounds usually contain only one type of alkali cations in-between the edge-shared octahedra layers. Herein, the ternary phase diagram $A_2Ni_2TeO_6$ (A = Li, Na, K) was explored through solid-state synthesis and new alkali-mixed compositions showing alternation of distinct alkali layers are obtained. Such intergrowth structures are synthesized either by single high-temperature treatment from raw chemicals or through reaction between layered precursors, the latter involving a solid-state process triggered at moderate temperatures.

The in-depth characterization of the multiple cationic orderings is performed by combining powder diffraction techniques (X-rays and neutrons), high-resolution TEM and solid-state NMR spectroscopy. In addition to the Ni/Te honeycomb ordering, alternation of lithium layers with sodium or potassium layers is observed for the compositions $(Li/Na)_2Ni_2TeO_6$ or $(Li/K)_2Ni_2TeO_6$, respectively. Crystal structure solving was achieved by stacking building blocks of the respective single alkali layered oxides and unveiled a complex out-of-plane ordering of honeycomb layers. Moreover, a solid-state reaction between $Li_2Ni_2TeO_6$ and $NaKNi_2TeO_6$ enables preparation of the new phase $Li_{\sim 1}Na_{\sim 0.5}K_{\sim 0.5}Ni_2TeO_6$, a unique example containing up to three alkali cations and exhibiting a more complex stacking with sodium and potassium cations occupying the same layer.

This investigation confirms that the chemical versatility of layered alkali transition metal compounds could also occur on the alkali layer. Following the research methodology described here, it should encourage to revisit the crystal chemistry of alkali transition metal layered materials by exploring alkali ions substitutions previously thought infeasible, in order to find out new alkali-mixed compositions.

Introduction

Solid-state chemists have long used cationic substitutions to take a simple chemical formula and expand the compositional range, with the aim of accessing new and interesting properties. In optimizing a new synthesis, they might modify the original pathway, either by tuning the mixing of the elements (solid-state grinding, hydrothermal, co-precipitation, sol-gel, etc.) or the thermal treatment. This history has been extensively applied to crystalline layered alkali transition metal oxides (A_xMO_2), a family of materials with a wide range of compositions with exciting chemical and physical characteristics. Such versatility originates from their layered crystallographic structure, often described as stacking of edge-sharing MO_6 octahedra layers sandwiching alkali layers. Chemical substitutions are often focused on the transition metal ions, owing to the very close ionic radii of many chemical elements that allows abundant mixing on the octahedral M site. A notable example is $LiCoO_2$, the standard lithium-ion battery electrode material, and its derivatives $Li(Ni,Mn,Co)O_2$ or $Li(Ni,Co,Al)O_2$ further designed to enhance the electrochemical performance, in which transition metals are randomly distributed.[1–3] For the particular 2:1 ratio in the transition metal layer, a honeycomb cationic ordering is often observed. The group of honeycomb layered oxides gathers fascinating features, such as electrochemical anionic redox for Li-rich compositions Li_2MO_3, high ionic diffusion in $Na_2M_2TeO_6$ compounds, particular magnetic properties or topological phase transition.[4]

The chemical richness of layered alkali transition metal oxides is also found on the alkali layer. Indeed, with the crystal structure depending on the nature of the alkali cation, different stackings sequences are induced by the alkali cations preferences for octahedral, tetrahedral or prismatic sites,[5] whereas for alkali-deficient compositions vacancy ordering can occur and sometimes induces unexpected physical properties, such as in the system Na_xCoO_2.[6–8] However, in contrast

to cationic substitutions inside the transition metal layer, cationic mixing within the alkali layer has not been deeply investigated so far. Given the substantial ionic size difference between lithium, sodium and potassium cations, at first glance combining at least two of them within the same layer might appear challenging. It is however not impossible, for example in the complete solid solutions $Li_{1-x}Na_xNi_{2/3}Sb_{1/3}O_2$ and $Li_{2-x}Na_xSnO_3$, in which single-phase compositions could be stabilized at room temperature through classic solid-state protocols with an efficient quench to the heat treatment.[9,10] Intergrowth of distinct alkali layers is another rare possibility to achieve alkali-mixed layered compositions. In 1994, Balsys and Davis combined O3-$LiCoO_2$ and P2-Na_xCoO_2 (following stacking nomenclature with letters accounting for the alkali site environment and numbers referring to the layers in the hexagonal cell[5]) and reported the composition OP4-$Li_xNa_yCoO_2$ with alternated layers of lithium and sodium cation. Here as well, a final quench is necessary to avoid phase segregation.[11–13] In 2021, the P2-type compound $NaKNi_2TeO_6$ was reported by the group of Masese. It contains both honeycomb ordering of the Ni/Te cations and alternate ordering of sodium and potassium layers along the hexagonal *c*-axis.[14] This material could be obtained directly from raw precursors, such as carbonates and oxides, but also in a two-step process through solid-state reaction between layered phases $Na_2Ni_2TeO_6$ and $K_2Ni_2TeO_6$. Interestingly here, alkali layers alternation seems thermodynamically stable and consequently $NaKNi_2TeO_6$ does not require quenching to be isolated at room temperature.[15]

In the search for new layered alkali-mixed compositions, herein we extended the space of investigation by also considering the metastable layered analogue $Li_2Ni_2TeO_6$[16,17] (Figure 1). Through a simple solid-state chemistry approach, we successfully prepared two new single-phase compositions $(Li/Na)_2Ni_2TeO_6$ and $(Li/K)_2Ni_2TeO_6$ for which the long-range alternation of

distinct alkali layers is characterized from powder diffraction techniques, although local range analyses reveal a more complex picture in certain regions of the crystallites. We also identified a third composition $Li_{\sim 1}Na_{\sim 0.5}K_{\sim 0.5}Ni_2TeO_6$ as the first example of layered alkali transition metal oxide containing the three alkali cations.

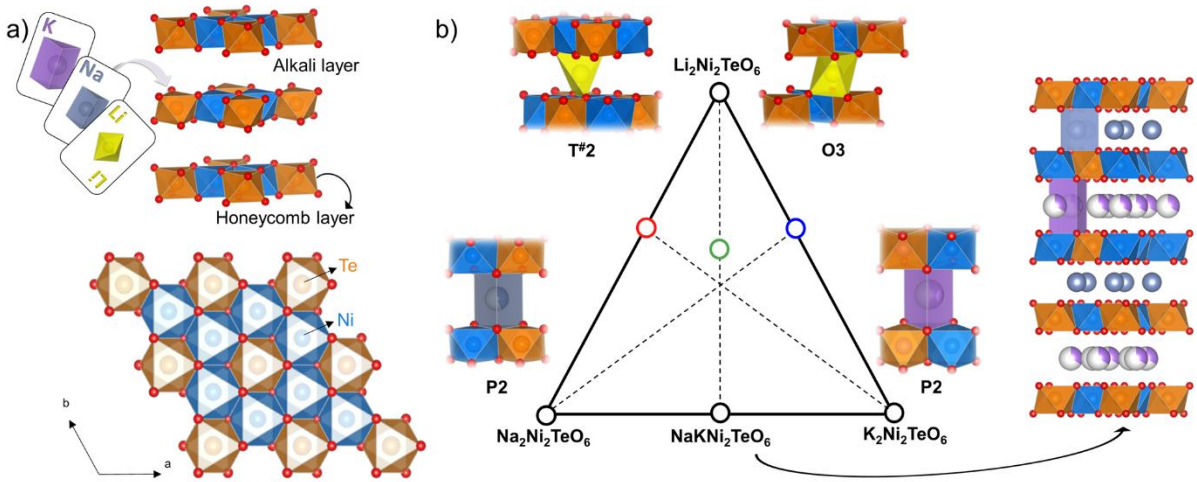

Figure 1. Crystal structure of the layered compounds $A_2Ni_2TeO_6$ (A = Li, Na, K) showing the alkali layers in-between the honeycomb Ni/Te slabs (a); ternary phase system highlighting the possible alkali site environments, with the continuous and dashed lines investigated in this work and circles indicating the single-phase alkali-mixed compositions (b).

In parallel, we scrutinized the synthesis of these alkali-ordered stackings by *in situ* powder diffraction techniques and revealed that their formation involves a classic nucleation/growth process, for which the triggering temperature can be significantly lowered by using single-alkali layered precursors. We believe that this solid-state synthesis pathway should be extended to revisit the crystal chemistry of alkali transition metal layered materials in order to find out new alkali-mixed compositions.

Results and Discussion

Between the P2-type compounds $Na_2Ni_2TeO_6$ and $K_2Ni_2TeO_6$ the thickness of the Ni/Te honeycomb layer does not evolve significantly. On the contrary the alkali layer is strongly influenced by the size of the alkali cations, and expands when potassium cations are considered.[18,19] These crystal features remain in $NaKNi_2TeO_6$, inducing an averaged value of the *c*-axis cell parameter and consequently and intermediate position of the (00l) diffraction peaks. Moreover, the alternation of distinct sodium and potassium layers implies a superstructure peak at low angle to account for this doubled periodicity along the hexagonal *c*-axis.[14,15] Keeping in mind how these stacked structures impact on the X-ray powder diffraction patterns, we sought for alkali-mixed layered phases in this system and initially investigated the compositions $Li_{2-x}Na_xNi_2TeO_6$ and $Li_{2-x}K_xNi_2TeO_6$ ($0 \leq x \leq 2$) through direct solid-state syntheses at 800 °C from raw chemicals, without any quenching at the end of the heat treatment. As displayed in the XRPD patterns of Figure 2, for $x = 2$ $Na_2Ni_2TeO_6$ and $K_2Ni_2TeO_6$ are expectedly obtained, with crystallographic features in line with previous works.[18,19] For $x = 0$, the significant intermixing occurring at high temperature between lithium and nickel cations unsurprisingly favors the formation of the orthorhombic polymorph of $Li_2Ni_2TeO_6$ instead of a layered one[16,17] (Figures S1-3 and Tables S1-3).

For intermediate compositions $Li_{2-x}Na_xNi_2TeO_6$ and $Li_{2-x}K_xNi_2TeO_6$, the two series of XRPD patterns are not characteristic of a solid-solution behavior. Instead, new diffraction peaks emerge and suggest a biphasic domain on both sides of the composition range. However, for $x = 0.8$ there is no more trace of $Li_2Ni_2TeO_6$ and $Na_2Ni_2TeO_6$ or $K_2Ni_2TeO_6$. The intermediate position

of the most intense peak and the presence of a superstructure peak at low angles suggest a single-phase layered compound with alternated layers of alkali elements. In the second series, the larger scattering difference between lithium and potassium cations explains the higher intensity of the superstructure peak. Corresponding chemical compositions have been determined as $Li_{1.1(1)}Na_{0.8(1)}Ni_{2.1(1)}Te_{0.9(1)}O_6$ and $Li_{1.1(1)}K_{0.6(1)}Ni_{1.9(1)}Te_{0.8(1)}O_6$ by ICP-AES analysis (Table S4), and will be shorten hereafter as $(Li/Na)_2Ni_2TeO_6$ and $(Li/K)Ni_2TeO_6$.

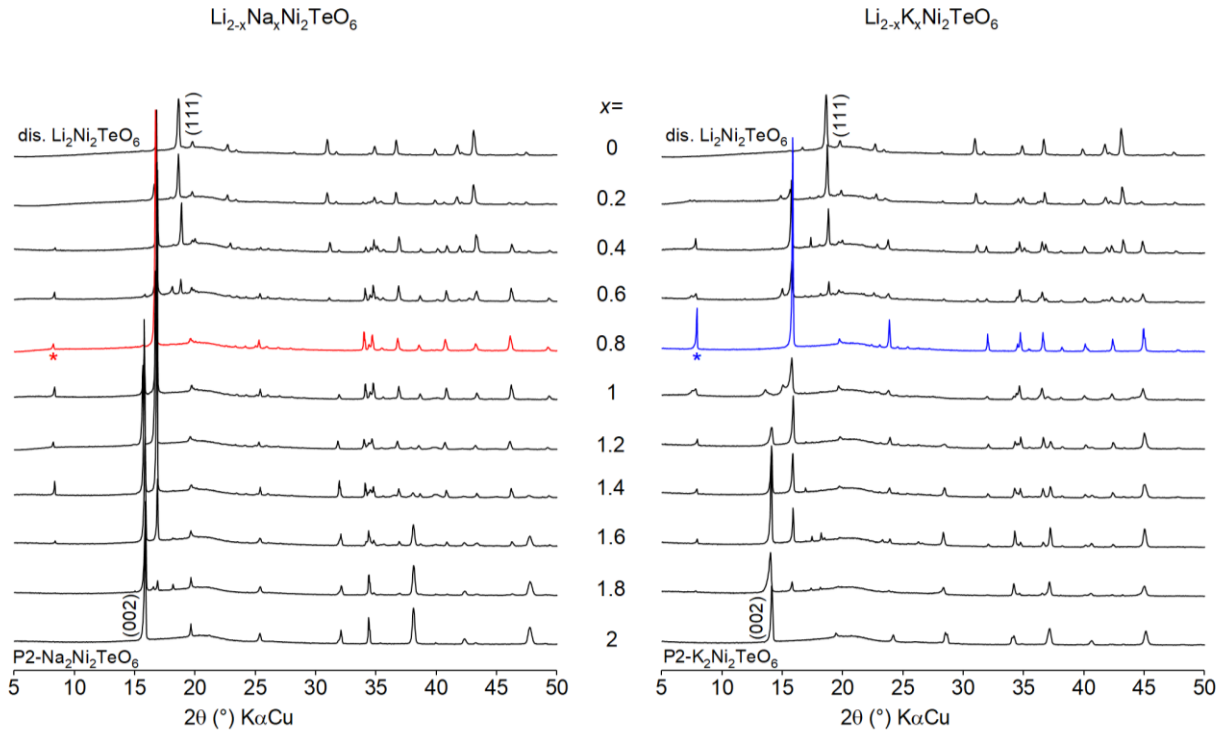

Figure 2. XRPD patterns for $Li_{2-x}Na_xNi_2TeO_6$ and $Li_{2-x}K_xNi_2TeO_6$ compositions collected after direct solid-state synthesis. End members are orthorhombic $Li_2Ni_2TeO_6$ (with Li/Ni intermixing), and P2-type $Na_2Ni_2TeO_6$ and $K_2Ni_2TeO_6$, respectively. For $x = 0.8$, a single-phase pattern is observed (colored patterns) and exhibits a low-angle superstructure peak (*) calling for alternation of distinct alkali layers along the hexagonal *c*-axis.

The game becomes more complex when up to three alkali cations are considered. All of our direct attempts for compositions $Li_{2-x-y}Na_xK_yNi_2TeO_6$ led to multiphasic products. Consequently, the synthesis protocol was modified by heating mixtures of layered precursors containing all the three alkali cations. In other words, we sought for solid-state reactions between a single-alkali layered precursor $A_2Ni_2TeO_6$ with an alkali-mixed precursor A'A"Ni_2TeO_6, following the inner lines of the ternary system shown in Figure 1b. It was not possible to obtain a single-phase product, neither with mixtures of $K_2Ni_2TeO_6$ and $(Li/Na)_2Ni_2TeO_6$, nor with mixtures of $Na_2Ni_2TeO_6$ and $(Li/K)_2Ni_2TeO_6$, although it was clear that some reactions occurred between the precursors (Figures S4-5). For the last series, the alkali-ordered $NaKNi_2TeO_6$ was mixed a layered polymorph of $Li_2Ni_2TeO_6$, obtained through topotactic ionic exchange from $Na_2Ni_2TeO_6$ and characterized by lithium ions in tetrahedral site ($T^{\#}2$-type stacking)[17] (Figure S6 and Table S5). XRPD patterns present a single-phase product only for an initial equimolar mixture, with here as well a unique intense peak at $2\theta = 15.8$ ° and a superstructure peak at low angles (Figure S7). The corresponding chemical composition was determined as $Li_{0.9(1)}Na_{0.5(1)}K_{0.4(1)}Ni_{2.0(1)}Te_{0.9(1)}O_6$ by ICP-AES, in fairly good agreement with a stoichiometric mixture of $Li_2Ni_2TeO_6$ and $NaKNi_2TeO_6$.

To summarize, the investigation of the ternary system reveals three single-phase alkali-mixed compositions, all adopting a layered structure characterized by an additional out-of-plane cationic ordering. At this stage, it is worth pointing out that these compositions are all obtained after a slow cooling and are thus thermodynamically stable, like the analogue $NaKNi_2TeO_6$. Secondly, it is interesting to see that the significant Li^+/Ni^{2+} intermixing leading to an orthorhombic form of $Li_2Ni_2TeO_6$ seems not to occur for the direct high-temperature synthesis of

$(Li/Na)_2Ni_2TeO_6$ and $(Li/K)_2Ni_2TeO_6$, when half of the lithium is replaced by bigger alkali cations.

To grasp further into the details of their crystal structure, we combined synchrotron X-ray powder diffraction (SXRPD) to get high-angular resolution patterns, and neutron powder diffraction (NPD) to better localize the light elements such as lithium. Assuming that the structural features of $(Li/K)_2Ni_2TeO_6$ and $(Li/Na)_2Ni_2TeO_6$ could be quite similar with those of the single-alkali compositions, especially the local symmetry of each alkali ions, SXRPD patterns were firstly refined by adapting the structural model of OP4-$Li_xNa_yCoO_2$,[11,12] with distinct layer of lithium ions (occupying octahedral sites) and sodium or potassium ones (in trigonal prismatic sites). In this model, the honeycomb arrangement between nickel and tellurium cations was not considered but averaged through a random distribution with relative 2/3 and 1/3 occupancies, respectively. The hexagonal cell parameters for $(Li/K)Ni_2TeO_6$ (a = 3.0016(1) Å, c = 22.3554(3) Å) and for $(Li/Na)Ni_2TeO_6$ (a = 2.9936(1) Å, c = 20.9744(8)) Å) match well with theoretical values calculated from the crystallographic features of the single-alkali compositions (for the c-axis parameters, 22.210 Å and 20.876 Å, respectively, Figures S8-9 and Tables S6-9).

Enlarged cells have been then considered to index more diffraction peaks. The hexagonal base was expanded firstly to $\sqrt{3}a \times \sqrt{3}a$ to take into account the Ni/Te honeycomb ordering; and it was then possible to index all the peaks by also tripling the c-axis parameter (Figure S10). However, all of our further structural refinement attempts using this cell were not satisfactory. Considering that stacking faults might occur in such intergrowth layered structure, like aperiodic gliding observed in the analog composition $NaKNi_2TeO_6$, and make unrealistic the determination

of a single space group using conventional crystal structure solving methods, we thus preferred to perform Rietveld refinements with a structural model built from a stacking block approach as offered by TOPAS-Academic software.[20] For $(Li/K)_2Ni_2TeO_6$, lithium and potassium building blocks were isolated from their respective parent phases (*i.e.* layered O3-$Li_2Ni_2TeO_6$ and P2-$K_2Ni_2TeO_6$) and superimposed along the *c*-axis according to different available stacking vectors (Figures S11-12 and Tables S10-11). A stack of twelve layers with perfect Li/K alternation was built in *P*1 symmetry to match with the cell parameters retrieved from the preliminary refinement work. The resulting OP12 structure gives a reasonable description of the main diffraction peaks but it does not suitably fit the superstructure peaks (Figure S13). We then hypothesized that 3*c* expansion was due to periodic translation of the honeycomb layers. Indeed, for a given $Li_2Ni_2TeO_6$ block, the next $K_2Ni_2TeO_6$ one has to be translated by (1/3, 0), (0, 1/3) or (-1/3, -1/3) in the (*a*,*b*) plane in order to create octahedral sites for lithium cations. If these three translations are set to occur by circular permutation, the superstructure peaks are perfectly described and Rietveld refinement of the SXRPD data gives a very good fit (Figure 3). A symmetry check was then performed on the latter model and space group $P3_121$ (n° 152) was identified, and both SXRPD and NPD data were refined accordingly. The occupancies of the different potassium sites were found to be strongly correlated to each other. We choose to avoid any erroneous conclusion regarding the in-plane potassium cations arrangement and hence opted for a uniform distribution model which gives a very satisfactory fit as well. Final cell parameters are $a = 5.1971(1)$ Å and $c = 67.0490(8)$ Å, and the chemical composition is estimated as $Li_{1.25}K_{0.75}Ni_2TeO_6$, in very good agreement with the nominal excess of lithium (Figure 2). Unsurprisingly, the values of the bond distances, 2.18 - 2.20 Å for Li – O and around 2.75 Å for K – O, are found in line with previous structural analyses of single-alkali compounds and

confirm that the alternated stacking of distinct alkali layers does not modify significantly the general crystal features. A similar approach has been applied to $(Li/Na)_2Ni_2TeO_6$ but the refinement was more difficult due to the presence of a $Na_2Ni_2TeO_6$ secondary phase in the analyzed sample (Figure S9).

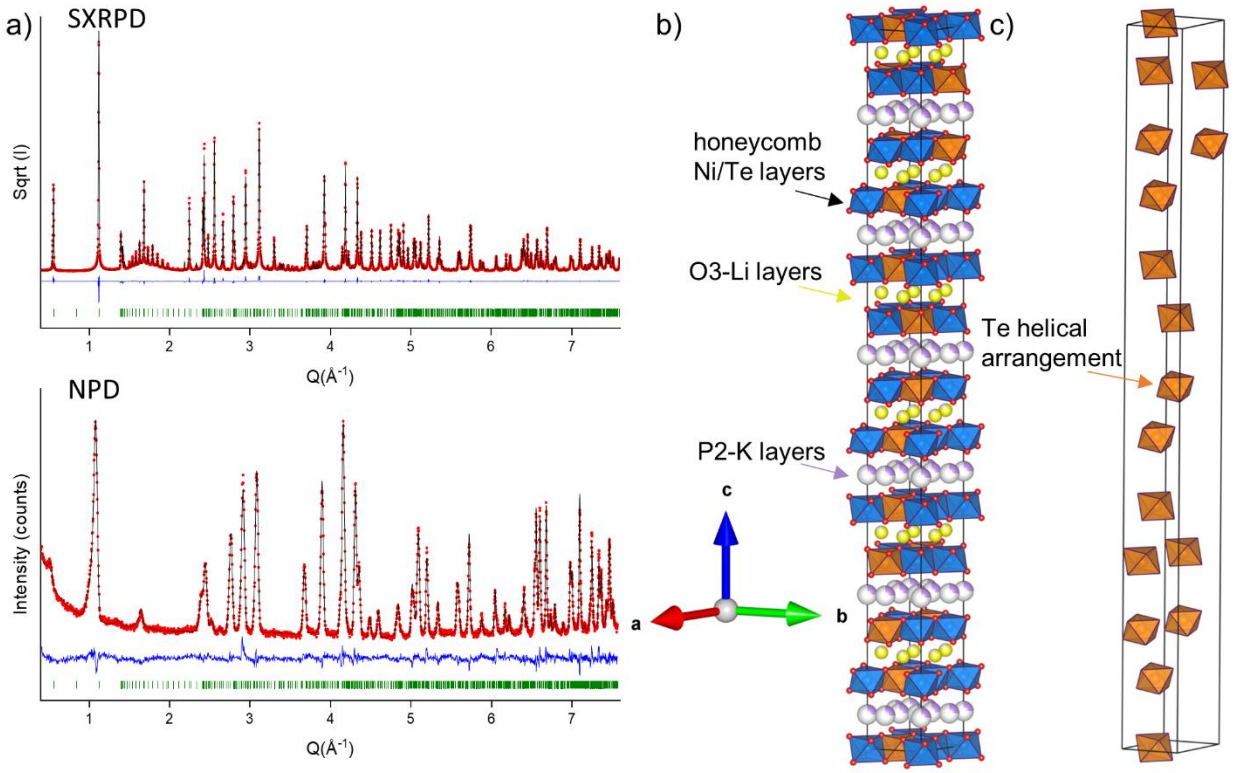

Figure 3. SXRPD and NPD Rietveld refinement for $(Li/K)_2Ni_2TeO_6$ using the structural model from TOPAS-Academic software (a); corresponding crystal structure showing the stacking sequence of the honeycomb blocks (b); focus on the helical arrangement of the TeO_6 polyhedra (c). The √I(counts) scale for the SXRPD pattern allows to picture the superstructure peaks and diffuse features especially around 1.7 $Å^{-1}$.

In parallel to powder diffraction techniques, high-resolution transmission electron microscopy (TEM) and ^{7}Li and ^{23}Na solid-state nuclear magnetic resonance (NMR) spectroscopy and have been carried out to investigate the structure at a local scale. Advanced high-resolution high-angle

annular dark-field scanning transmission electron microscopy (HAADF-STEM) and electron diffraction (ED) have been performed for $(Li/K)_2Ni_2TeO_6$. ED patterns collected for main zone axis can be fully indexed with a hexagonal cell especially with a *c*-axis parameter around 67 Å, in very good agreement with the above-described structural refinement. Both the in-plane honeycomb cationic ordering and the general layered structure along *c*-axis are confirmed on the [001] and [100] HAADF-STEM images (respectively in Figure 4a and b). In particular, inside the brightest layers, it is possible to distinguish Te and Ni atoms (Z = 52 and 28, respectively), whereas dark lines stand for the alkali cations, the latter being visible on annular bright field STEM images (Figure S14). Given the respective atomic weight of lithium and potassium (Z = 3 and 19), but also the difference thickness of each layer, the darker and thicker interslab space on HAADF-STEM images corresponds to potassium layers. Finally, it worth pointing out that crystalline areas with perfect alternation of distinct alkali layers, like what was observed on $NaKNi_2TeO_6$,[14] could coexist with faulted domains characterized by a significant stacking disorder, as shown on two different enlarged views. Considering the TEM analysis revealing a possible disorder between lithium and potassium layers in localized areas, we took advantage of the structural refinement approach described above to induce stacking faults in the layered structure of $(Li/K)Ni_2TeO_6$, such as an imperfect Li/K alternation or a random translation of the transition honeycomb slabs, to evaluate how they might influence the SXRPD patterns. Consequently, two models were built by stacking 500 individual layers and assigning different probabilities that a stacking fault occurs. None of this stacking defects were found to be the origin of these unusual superstructure peaks centered at 1.7 $Å^{-1}$. Instead of that, they likely contribute to a diffuse scattering (Figures S15-16). This simulation demonstrates that stacking defects observed by TEM should be actually scarce in the whole material.

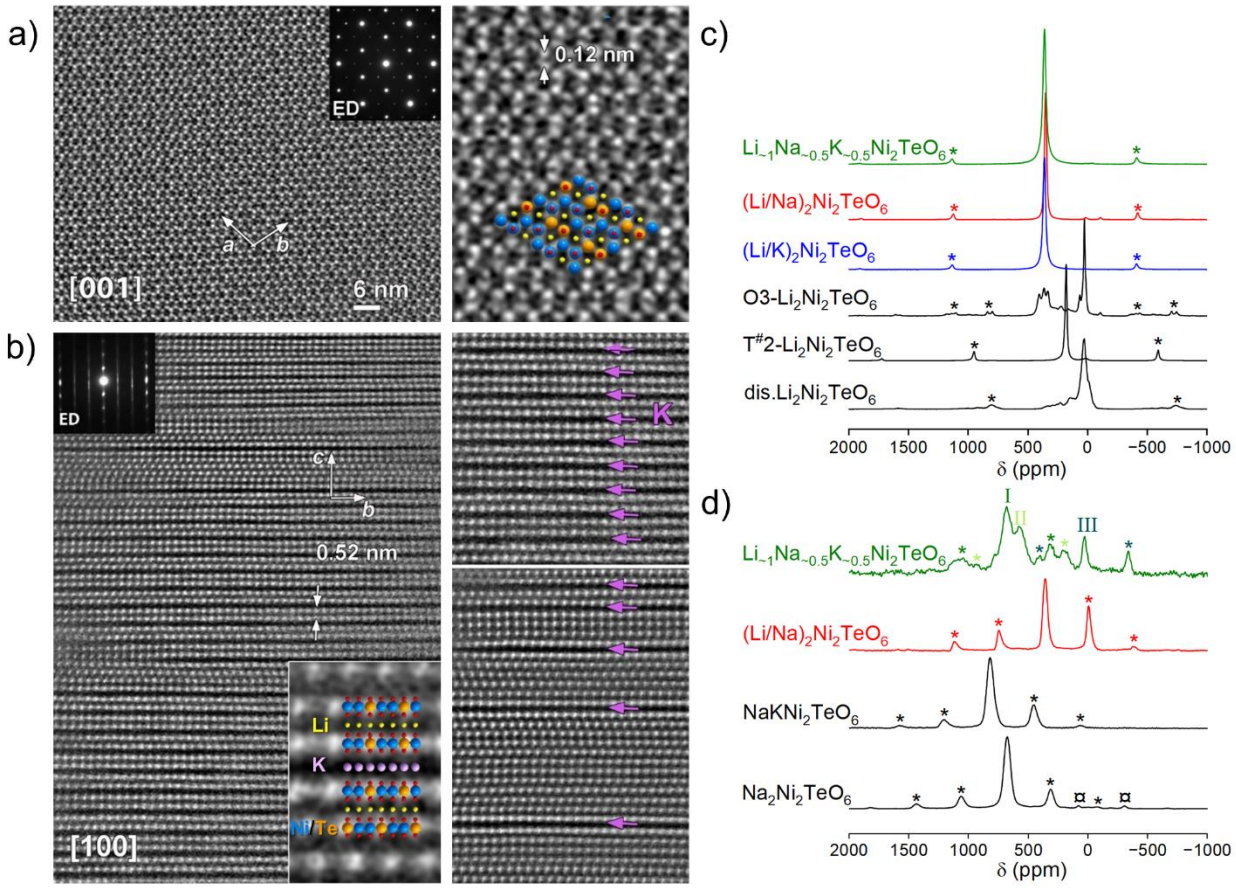

Figure 4. High-resolution HAADF-STEM and ED analysis on $(Li/K)_2Ni_2TeO_6$ especially highlighting the ordered and disordered on the alternation of lithium and potassium layers (a-b); ^{7}Li and ^{23}Na solid-state MAS-NMR analysis of the alkali-mixed compositions with comparison with reference layered materials and * for the spinning bands (c-d);

^{7}Li NMR spectra are compared in Figure 4c. An isotropic signal at 187 ppm is observed for $T^{\#}2\text{-}Li_2Ni_2TeO_6$, *i.e.* the polymorph obtained directly after ionic-exchange from $Na_2Ni_2TeO_6$. Such a large shift results from Fermi contact interaction occurring between the Ni^{2+} paramagnetic ions and the ^{7}Li nuclei. As a single signal is seen, it certainly accounts for a high lithium ion mobility in the interslab space leading to an average position of all possible lithium environments with respect to the Ni/Te position. The other layered reference $O3\text{-}Li_2Ni_2TeO_6$,

obtained by heating the $T^{\#}2$ polymorph (Figure S17 and Table S12), exhibits a more complex spectrum, with first a significant contribution at 26 ppm which could indicate the beginning of Li/Ni intermixing, according to what is observed for the thermodynamically stable disordered $Li_2Ni_2TeO_6$ polymorph obtained by a direct solid-state synthesis. The spectrum also shows three broad contributions between 334 and 405 ppm, which might be attributed to lithium ions in octahedral sites. The very similar spectra observed for the three alkali-mixed compositions are characterized by a unique isotropic contribution around $\delta = 350$ ppm and then must be interpreted by a single type of lithium octahedral sites, with here as well a high ionic mobility in the interslab leading to a unique average position. The absence of signal at 26 ppm confirms the absence of Li/Ni intermixing in the alkali-mixed compositions. ^{23}Na NMR spectra of reference compounds $Na_2Ni_2TeO_6$ and $NaKNi_2TeO_6$ both exhibit a major isotropic peak, respectively at $\delta = 677$ and 820 ppm (Figure 4d). Such large shifts are due to the Fermi contact interaction occurring between the Ni^{2+} paramagnetic ions and the ^{23}Na nuclei. Although different sodium prismatic sites are possible in P2-type honeycomb structure, whether they share either faces or edges with NiO_6 and TeO_6 octahedra above and below, the presence of a unique signal was previously explained by the high mobility of sodium cations which averages the signal.[21,22] The difference in the peak shift was also rationalized through DFT calculations and explained by distinct stacking sequences of the Ni/Te honeycomb layers through each sodium layers.[15] A very close spectrum is observed for $(Li/Na)_2Ni_2TeO_6$, confirming the distinct P2-type layers of sodium cations, however with a significantly weak peak displacement (358 ppm). Such weaker Fermi contact shift can come from either longer $Na-O$ distances implying weaker orbital overlap and thus weaker spin transfer from Ni^{2+} ions to Na nuclei, or a particular sequences of the Ni/Te layers relative to the positions of sodium cations.

For the third composition containing the three alkali cations, sodium and potassium ones were initially assumed to lie inside distinct layers, as random distribution within the alkali layer was found thermodynamically not favored in the analogue material $NaKNi_2TeO_6$.[15] Therefore a complex stacking sequence Li/Na/Li/K was designed theoretically, with a corresponding *c*-axis parameter around 21.54 Å. However, a significantly higher value of 22.427(1) Å was determined from profile matching refinement and consequently questioned the initial structure hypothesis (Figure S18 and Tables S8-9). In parallel, the ^{23}Na NMR analysis revealed a more complex spectrum for $LiNa_{\sim 0.5}K_{\sim 0.5}Ni_2TeO_6$, compare to those of $(Li/Na)_2Ni_2TeO_6$ and $NaKNi_2TeO_6$, with at least three broad and overlapping contributions. While the major one is really close to what is observed for $Na_2Ni_2TeO_6$ and must consequently be attributed to mobile sodium ions in similar environment, the two others call for additional environments (Figure 4d). No exchange at the NMR scale is observed between the three contributions, making possible a significant structural disorder within the sodium layer.

Considering both the strong similarities between the SXRPD patterns, we hypothesized that the layered structure is composed of only two types of alkali layers: a first one with lithium cations and the second one with a random distribution of sodium and potassium cations lying in trigonal prismatic sites. The thickness of this layer is governed by the bigger potassium cations and induces an experimental value of the *c*-axis parameter somehow very close to the one of $(Li/K)_2Ni_2TeO_6$. In addition, such arrangement could also explain the structural disorder observed by ^{23}Na NMR. To support this hypothesis, structural refinement through the building block approach were also attempted with either a "segregated" or a "mixed" model, *i.e.* following Li/Na/Li/K or Li/(Na,K) sequences, respectively (Figure S19 and Table S13). The

agreement factor was slightly better in the latter case. Furthermore, the "segregated" stacked model was found to possess some very small Bragg peaks that do not exist in the experimental diffraction pattern and which are hypothesized to originate from the symmetry lowering due to the presence of distinct Na and K layers (Figure S20). Consequently, the model consisting of mixed (Na,K) layers was validated and finally refined against SXRPD and NPD patterns with the $P3_121$ space group. Final cell parameters are $a = 5.1985(1)$ Å and $c = 67.258(2)$ Å, and the chemical composition is estimated as $Li_{1.05}Na_{0.48}K_{0.48}Ni_2TeO_6$ (Figure S21).

The first section of our investigation demonstrated that alkali-ordered layered oxides could be obtained by a direct solid-state reaction either directly from raw precursors or through the combination of as-prepared single-alkali layered compounds. Thus, the latter could reasonably act as intermediates in case of a straightforward synthesis. To verify that, we scrutinized by laboratory XRPD the formation of $(Li/K)_2Ni_2TeO_6$ from raw precursors (alkali carbonates, nickel and tellurium oxides). The main diffraction peak of the alkali-mixed composition starts to be observed around 550 °C; however with no trace of $Li_2Ni_2TeO_6$ and $K_2Ni_2TeO_6$ at lower temperatures (Figure 5a). Consequently, $(Li/K)_2Ni_2TeO_6$ seems to be formed directly. At this point, it is worth recalling that $NaKNi_2TeO_6$ could be also obtained by heating a mixture of layered parents $Na_2Ni_2TeO_6$ and $K_2Ni_2TeO_6$ at 200 °C only.[15] Given the high ionic conductivity of both sodium and potassium in these P2-type layered compounds, a simultaneous ionic exchange between the precursors was proposed to explain this relatively low temperature for a solid-state reaction, but not confirmed experimentally. We thus decided to probe the formation of the alkali-mixed compositions by SXRPD by heating up to 600 °C quartz capillaries containing the corresponding mixtures of single-alkali layered precursors (Figure 5b).

Focusing first on $(Li/K)_2Ni_2TeO_6$, the (00l) peaks of the pre-cursors progressively shift towards low angles and simultaneously decrease in intensity, and the main peak of the alkali-mixed compositions becomes detectable at 310 °C or 130 °C whether the lithium precursor is O3- or $T^{\#}2\text{-}Li_2Ni_2TeO_6$, respectively. The regular displacement of the precursors' peak with increasing temperature is attributed to thermal lattice expansion. These observations do not support the firstly hypothesized mechanism based on topotactic Li^+/K^+ simultaneous exchanges, for which the significant evolution of alkali layer thickness for each precursors would have induced a progressive gathering of these two peaks (Figure S22). On the contrary, the progressive disappearance of the precursors together with the apparition of the peak of the alkali-mixed (Li/K) stacking tends to validate a classical nucleation/growth mechanism. In comparison with the direct solid-state synthesis from an initial mixture of carbonates and oxides, the formation of $(Li/K)_2Ni_2TeO_6$ starts at very low temperatures, which makes sense considering the very close crystallographic features of the layered precursors. In addition, the process seems also triggered by the intrinsic mobility of alkali ions inside each layered precursor, as the lowest temperature formation is observed with the $T^{\#}2\text{-}Li_2Ni_2TeO_6$ as precursor. At a glance, the formation of the other ordered stackings (Li/Na) or (Na/K) follows the same pathway with a nucleation/growth process initiated below 200 °C thanks to the high alkali cations mobility in $T^{\#}2\text{-}Li_2Ni_2TeO_6$, as well as in the P2-type sodium and potassium analogues.[18,19] However, with a second look it clearly appears that the peaks of these two latter precursors evolve slightly differently at high temperature. Indeed, although still decreasing in intensity, the peaks start to shift in the opposite direction despite the increasing temperature. This could indicate a minor contraction of the *c*-axis parameter, which cannot fully discard a weak insertion of the smaller alkali ions (Li^+ in $Na_2Ni_2TeO_6$, or Na^+ in $K_2Ni_2TeO_6$, respectively).

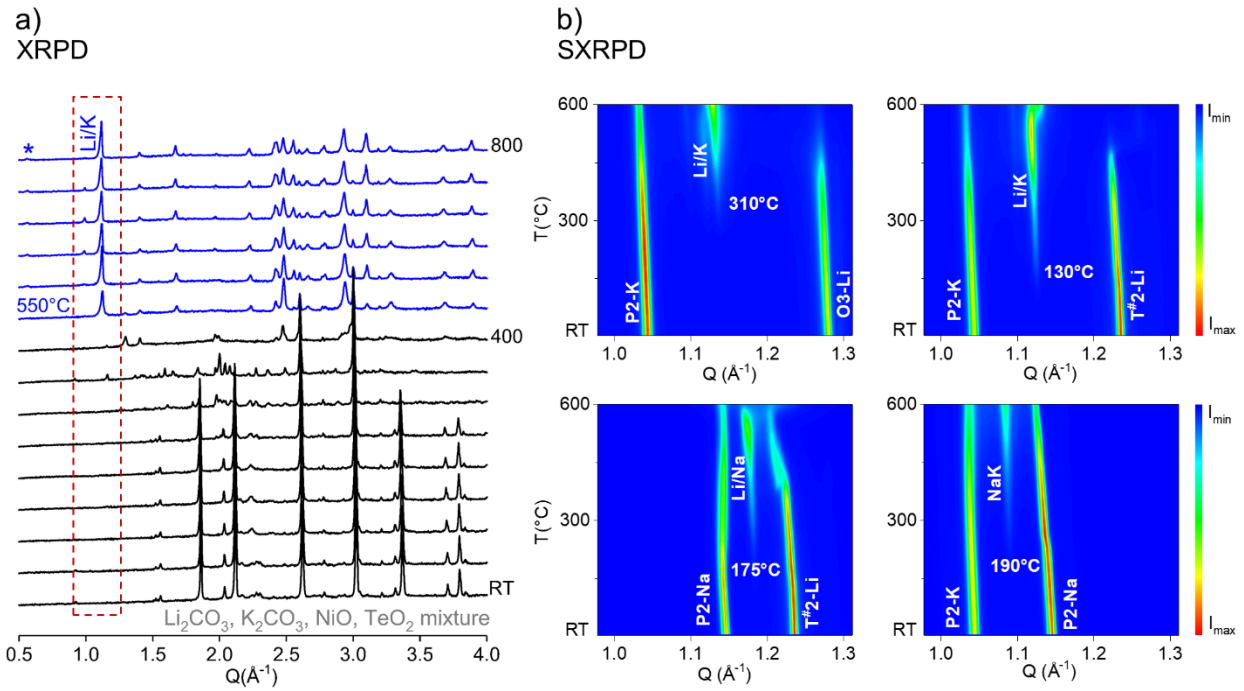

Figure 5. XRPD patterns collected in temperature to follow the synthesis of $(Li/K)_2Ni_2TeO_6$ from raw precursors (a); SXRPD patterns revealing the low-temperature formation of $(Li/K)_2Ni_2TeO_6$ (top), $(Li/Na)_2Ni_2TeO_6$ and $NaKNi_2TeO_6$ (bottom) when single-alkali layered $A_2Ni_2TeO_6$ (A = Li, Na or K) are used as precursors (b).

Conclusion

Exploring the ternary phase diagram $A_2Ni_2TeO_6$ (A = Li, Na and K) by solid-state synthesis allowed us to discover and investigate three new highly crystalline layered honeycomb oxides exhibiting unique alternation of alkali layers. Although layered $Li_2Ni_2TeO_6$ is usually only obtained by ionic exchange, we successfully stabilized layered compositions $(Li/K)_2Ni_2TeO_6$ and $(Li/Na)_2Ni_2TeO_6$ after a single heat treatment. For both of them, the alternation of distinct alkali layers was firstly assumed theoretically and then experimentally verified by powder diffraction techniques. Similarly to the layered parent phases, whereas lithium ions occupy octahedral sites both sodium and potassium cations lie in trigonal prismatic positions. Nevertheless, high-

resolution TEM revealed that the alkali layers alternation could be significantly altered at the atomic scale. In a second step, we used these alkali-ordered layered compounds and combined them with a single-alkali precursors to play with more alkali cations. We thus discovered that the solid-solid reaction between $Li_2Ni_2TeO_6$ and $NaKNi_2TeO_6$ enables formation of a single-phase composition containing up to three alkali ions inside the layered structure, with sodium and potassium cations unexpectedly sharing the same layer.

Although layered alkali transition metal compounds have been known for decades and a wide range of cationic substitutions have been already attempted, especially in the search for promising compositions for positive electrode materials in rechargeable metal-ion batteries, our investigation confirms that there is still room for discovering new compositions especially by combining multiple alkali cations. In that case, a fine structural analysis combining synchrotron X-rays and neutron powder diffraction is required to understand where all the alkali ions are. Playing with several alkali layers obviously multiplies the gliding possibilities. We proposed a pertinent way to make use of chemical knowledge, such as alkali ion coordination preferences and the rigidity of the layers, to solve the crystal structure and assess the impact of stacking faults on the SXRPD via supercell simulations of fault types observed in the TEM.

Whereas most of the alkali-mixed compositions could be obtained by a direct solid-state protocol, our work highlights that combining layered precursors could sometimes be an interesting pathway to reach higher purity or even to access new compositions. Very interestingly, in this case the formation of the alkali-ordered stacking could be triggered at very moderate temperatures. We believe that such a low temperature range of solid-state transition, applied to other layered alkali transition metal oxides, or more generally chalcogenides, could be of interest in terms of ionic conductivity. This work and the underlying solid-state synthesis

methodology should stimulate to revisit some layered alkali transition metal systems, supposed perfectly known for a long time, in order to discover new alkali-mixed compositions with perhaps intriguing properties.

Methods

Materials synthesis. Layered $Na_2Ni_2TeO_6$ and $K_2Ni_2TeO_6$ and disordered $Li_2Ni_2TeO_6$ were synthesized through a conventional solid-state reaction adapting procedures from previous reports.[17–19] Dried alkali carbonates (Na_2CO_3 (Alfa Aesar, 99.95 %), K_2CO_3 (Sigma-Aldrich, 99.995 %), Li_2CO_3 (Alfa Aesar, 99.9 %)), nickel oxide (NiO, Thermo Scientific, 99 %) and tellurium oxide (TeO_2, Thermo Scientific, 99.99 %), were mixed in stoichiometric proportions and grinded in an agate mortar inside the glovebox, then pelletized and placed in a gold crucible before heating at 800 °C. For $K_2Ni_2TeO_6$ a 10% nominal excess of potassium carbonate was added to balance high-temperature loss. The heating/cooling rate was 2 °Cmin^{-1} and the dwelling time was 9 h for $Na_2Ni_2TeO_6$ and $Li_2Ni_2TeO_6$ and 24 h for $K_2Ni_2TeO_6$. Layered $Li_2Ni_2TeO_6$ was prepared following a 2-steps synthesis, as a matter of fact, the conventional solid-state reaction leads to a disordered $Li_2Ni_2TeO_6$.[17] $T^{\#}2$-$Li_2Ni_2TeO_6$ was obtained by ion exchange in molten salt by adapting the reported process. A mixture of $Na_2Ni_2TeO_6$ and 10 times the stoichiometric weight of anhydrous lithium nitrate ($LiNO_3$, Thermo Scientific, 99 %) was heated in a porcelain crucible at 300 °C for 5 h (5 °C.min^{-1} heating rate and slow cooling to room temperature under air). Residual $LiNO_3$ and $NaNO_3$ contained in the resulting product were dissolved through sonication with deionized water before vacuum filtration and washing with deionized water and ethanol. The filtration residue was dried in an oven at 60°C overnight. Heating the resulting layered $T^{\#}2$-$Li_2Ni_2TeO_6$ led to the formation of the layered O3-$Li_2Ni_2TeO_6$ polymorph (800 °C

for 9h with 5 °C heating/cooling rate under air). Different $Li_{2-x-y}Na_xK_yNi_2TeO_6$ compositions were also attempted by direct solid-state synthesis from reactants, with 24 h heat treatments at 800 °C with a 2 °C.min^{-1} heating and cooling rate. In parallel, alkali-mixed compositions with the general formula A'A"Ni_2TeO_6 (A' and A" being Li, Na or K) were obtained by combining $Na_2Ni_2TeO_6$, $K_2Ni_2TeO_6$ and/or T$^{\#}$2-$Li_2Ni_2TeO_6$ layered precursors in stoichiometric proportions. The mixed precursors powders where pressed into pellets and heated at 800 °C for 9 hours with a 2 °C.min^{-1} heating and cooling rate. Finally, solid-state reactions between $A_2Ni_2TeO_6$ single-alkali precursors and A'A"Ni_2TeO_6 mixed-alkali precursors have been attempted to gather up to three alkali cations, following the previously described methodology.

Materials characterization. Laboratory X-ray powder diffraction (XRPD) measurements were performed in order to validate the formation of the targeted compositions. The patterns were collected using a Panalytical X'Pert Spinner Reflection diffractometer in an angular range going from 5 to 80 °, with a step of 0.033 ° and a 150 to 165 s counting time per step. The diffractometer operating in a θ/θ Bragg-Brentano geometry is equipped with a Cu X-ray source (λKα = 1.5406 Å). Synchrotron X-ray powder diffraction (SXRPD) data were collected on BL04_MSPD beamline at ALBA (Cerdanyola del Vallés, Spain) in transmission geometry with a wavelength of λ = 0.4142 Å.[23] All the samples were sealed, under argon inside a glovebox, in 0.7 mm quartz capillary tubes. Neutron powder diffraction (NPD) was performed at room temperature on the ECHIDNA high-resolution powder diffractometer[24] (1.622 Å wavelength) at ANSTO (Lucas Heights, Australia) for the $Li_2Ni_2TeO_6$, $Na_2Ni_2TeO_6$, $K_2Ni_2TeO_6$ and $(Li/K)_2Ni_2TeO_6$, and on the D2B high-resolution powder diffractometer (1.594 Å wavelength) at Institut Laue Langevin (Grenoble, France) for $(Li/Na)_2Ni_2TeO_6$ and $Li_{\sim1}Na_{\sim0.5}K_{\sim0.5}Ni_2TeO_6$. In each case vanadium tubes were used and filled in a glovebox. Profile matching and Rietveld

refinement were completed using FullProf and TOPAS-Academic, as the case may be. ^{7}Li magic-angle spinning (MAS) NMR spectra were recorded on a Bruker Avance III spectrometer, equipped with a 2.35 T widebore magnet (operating at the Larmor frequency of 38.93 MHz for ^{7}Li), using a standard Bruker 2.5 mm MAS probe. Powder samples were packed in zirconia rotors inside a glovebox under argon. The spinning frequency was 30 kHz for all the recorded spectra, the spectral width was set to 0.5 MHz and the recycle time of 0.5 s was used, long enough to avoid T1 saturation effects. A Hahn echo pulse sequence (π/2-delay-π) was applied with 2 μs π/2 pulse length and an average acquisition time of 0.01 s. Chemical shifts are referenced to an aqueous 1 M LiCl solution at 0 ppm. ^{23}Na MAS NMR spectra were recorded on a Bruker Avance 300 MHz spectrometer, equipped with a 7.05 T widebore magnet (operating at the Larmor frequency of 79.4 MHz for ^{23}Na), using a standard Bruker 2.5 mm MAS probe. The samples were packed in zirconia rotors inside a glovebox under argon. The spinning frequency was 30 kHz for all the spectra and a recycle time of 0.5 s was used, long enough to avoid T1 saturation effects. The spectral width was set to 1 MHz and a Hahn echo pulse sequence (π/2-delay-π) was applied with a 2 μs π/2 pulse length and an average acquisition time of 0.005 s for each case. Chemical shifts are referenced relative to an aqueous 0.1 M NaCl solution at 0 ppm. Transmission electron microscopy (TEM) including electron diffraction (ED) and high angle annular dark field scanning TEM (HAADF–STEM), annular bright field scanning TEM (ABF–STEM), and electron energy loss spectroscopy (EELS) experiments were performed using an aberration double–corrected JEM ARM200F microscope operated at 200 kV and equipped with a CENTURIO EDX detector, Orius Gatan CCD camera and GIF Quantum spectrometer. TEM samples were prepared by grinding the materials in an agate mortar with ethanol and depositing the obtained suspension on a Ni–carbon holey grid.

Supporting Information

SXRPD and NPD patterns and structural parameters for $Li_2Ni_2TeO_6$, $Na_2Ni_2TeO_6$ and $K_2Ni_2TeO_6$; additional high-resolution TEM images for $(Li/K)_2Ni_2TeO_6$; ICP-AES analysis; XRPD and SXRPD patterns for the compositions $Li_{1-x}Na_{1-x}K_{2x}Ni_2TeO_6$, $Li_{1-x}Na_{2x}K_{1-x}Ni_2TeO_6$, $Li_{2-x}Na_{x/2}K_{x/2}Ni_2TeO_6$; structural refinement attempts for the alkali-ordered layered compositions, details on the structural refinement through the TOPAS-Academic approach; crystallographic information file for $(Li/K)_2Ni_2TeO_6$ and $Li_{\sim 1}Na_{\sim 0.5}K_{\sim 0.5}Ni_2TeO_6$.

Acknowledgements

CELLS-ALBA is acknowledged for granting beamtime through academic proposal system (proposal ID 2022085941).

Data Availability Statement

The data that support the findings of this study are available from the corresponding author upon reasonable request. Neutron diffraction data performed at ILL at available at: https://doi.org/10.5291/ILL-DATA.5-22-806.

Corresponding Author Information

Dr. Romain Berthelot: romain.berthelot@umontpellier.fr

Authors Contribution

E.M.M. carried out the solid-state syntheses and the characterizations of the powder samples; E.M.M., B.F., G.R., R.W. and S.C. conducted the structural analysis; M.A. and E.S. collected the NPD data; F.F. collected the SXRPD; O.L. and E.G. conducted the TEM investigation; P.S.C. and D.C. carried out the NMR study; E.M.M. and R.B. wrote the manuscript and all authors discussed the experiments and final manuscript; R.B. supervised the overall investigation.

References

(1) Mizushima, K.; Jones, P. C.; Wiseman, P. J.; Goodenough, J. B. Li_xCoO_2 (0<x<-1): A New Cathode Material for Batteries of High Energy Density. *Mater. Res. Bull.* **1980**, *15* (6), 783–789.

(2) Abakumov, A. M.; Fedotov, S. S.; Antipov, E. V; Tarascon, J.-M. Solid State Chemistry for

Developing Better Metal-Ion Batteries. *Nat. Commun.* **2020**, *11* (1), 4976. https://doi.org/10.1038/s41467-020-18736-7.
(3) Li, M.; Lu, J.; Chen, Z.; Amine, K. 30 Years of Lithium-Ion Batteries. *Adv. Mater.* **2018**, *30* (33), 1800561. https://doi.org/https://doi.org/10.1002/adma.201800561.
(4) Kanyolo, G. M.; Masese, T.; Matsubara, N.; Chen, C.-Y.; Rizell, J.; Huang, Z.-D.; Sassa, Y.; Månsson, M.; Senoh, H.; Matsumoto, H. Honeycomb Layered Oxides: Structure, Energy Storage, Transport, Topology and Relevant Insights. *Chem. Soc. Rev.* **2021**, *50* (6), 3990–4030. https://doi.org/10.1039/D0CS00320D.
(5) Delmas, C.; Fouassier, C.; Hagenmuller, P. Structural Classification and Properties of the Layered Oxides. *Phys. B+C* **1980**, *99* (1–4), 81–85. https://doi.org/10.1016/0378-4363(80)90214-4.
(6) Chou, F. C.; Chu, M.-W.; Shu, G. J.; Huang, F.-T.; Pai, W. W.; Sheu, H. S.; Lee, P. A. Sodium Ion Ordering and Vacancy Cluster Formation in Na_xCoO_2 (X=0.71 and 0.84) Single Crystals by Synchrotron X-Ray Diffraction. *Phys. Rev. Lett.* **2008**, *101* (12), 127404.
(7) Huang, Q.; Foo, M. L.; Lynn, J. W.; Zandbergen, H. W.; Lawes, G.; Wang, Y.; Toby, B. H.; Ramirez, A. P.; Ong, N. P.; Cava, R. J. Low Temperature Phase Transitions and Crystal Structure of $Na_{0.5}CoO_2$. *J. Phys. Condens. Matter* **2004**, *16* (32), 5803–5814.
(8) Roger, M.; Morris, D. J. P.; Tennant, D. A.; Gutmann, M. J.; Goff, J. P.; Hoffmann, J.-U.; Feyerherm, R.; Dudzik, E.; Prabhakaran, D.; Boothroyd, A. T.; Shannon, N.; Lake, B.; Deen, P. P. Patterning of Sodium Ions and the Control of Electrons in Sodium Cobaltate. *Nature* **2007**, *445* (7128), 631–634.
(9) Vallée, C.; Saubanère, M.; Sanz-Camacho, P.; Biecher, Y.; Fraisse, B.; Suard, E.; Rousse, G.; Carlier, D.; Berthelot, R. Alkali-Glass Behavior in Honeycomb-Type Layered $Li_{3-x}Na_xNi_2SbO_6$ Solid Solution. *Inorg. Chem.* **2019**, *58* (17). https://doi.org/10.1021/acs.inorgchem.9b01385.
(10) Berthelot, R.; Crobu, C.; Mumba Mpanga, E.; Fraisse, B.; Doublet, M.-L. Rationalizing the Alkali Ions Distribution along the Honeycomb Layered $(Li,Na)_2SnO_3$ Pseudo Solid Solution. *Prog. Solid State Chem.* **2023**, *70*, 100403. https://doi.org/https://doi.org/10.1016/j.progsolidstchem.2023.100403.
(11) Balsys, R. J.; Lindsay Davis, R. The Structure of $Li_{0.43}Na_{0.36}CoO_{1.96}$ Using Neutron Powder Diffraction. *Solid State Ionics* **1994**, *69* (1), 69–74. https://doi.org/https://doi.org/10.1016/0167-2738(94)90451-0.
(12) Berthelot, R.; Pollet, M.; Carlier, D.; Delmas, C. Reinvestigation of the OP4-$(Li/Na)CoO_2$-Layered System and First Evidence of the $(Li/Na/Na)CoO_2$ Phase with OPP9 Oxygen Stacking. *Inorg. Chem.* **2011**, *50* (6). https://doi.org/10.1021/ic102218w.
(13) Biecher, Y.; Smiley, D. L.; Guignard, M.; Fauth, F.; Berthelot, R.; Delmas, C.; Goward, G. R.; Carlier, D. Original Layered OP4-$(Li,Na)_xCoO_2$ Phase: Insights on Its Structure, Electronic Structure, and Dynamics from Solid State NMR. *Inorg. Chem.* **2020**, *59* (8), 5339–5349. https://doi.org/10.1021/acs.inorgchem.9b03417.
(14) Masese, T.; Miyazaki, Y.; Rizell, J.; Kanyolo, G. M.; Chen, C.-Y.; Ubukata, H.; Kubota, K.; Sau, K.; Ikeshoji, T.; Huang, Z.-D.; et al. Mixed Alkali-Ion Transport and Storage in Atomic-Disordered Honeycomb Layered $NaKNi_2TeO_6$. *Nat. Commun.* **2021**, *12* (1), 4660. https://doi.org/10.1038/s41467-021-24694-5.
(15) Berthelot, R.; Serrano-Sevillano, J.; Fraisse, B.; Fauth, F.; Weill, F.; Laurencin, D.; Casas-Cabanas, M.; Carlier, D.; Rousse, G.; Doublet, M.-L. Stacking Versatility in Alkali-Mixed Honeycomb Layered $NaKNi_2TeO_6$. *Inorg. Chem.* **2021**, *60* (18), 14310–14317. https://doi.org/10.1021/acs.inorgchem.1c01876.
(16) Kumar, V.; Gupta, A.; Uma, S. Formation of Honeycomb Ordered Monoclinic $Li_2M_2TeO_6$ (M = Cu, Ni) and Disordered Orthorhombic $Li_2Ni_2TeO_6$ Oxides. *Dalt. Trans.* **2013**, *42* (42), 14992–14998. https://doi.org/10.1039/c3dt51604k.
(17) Grundish, N. S.; Seymour, I. D.; Henkelman, G.; Goodenough, J. B. Electrochemical Properties of Three $Li_2Ni_2TeO_6$ Structural Polymorphs. *Chem. Mater.* **2019**, *31* (22), 9379–9388. https://doi.org/10.1021/acs.chemmater.9b02956.

(18) Evstigneeva, M. A.; Nalbandyan, V. B.; Petrenko, A. A.; Medvedev, B. S.; Kataev, A. A. A New Family of Fast Sodium Ion Conductors: $Na_2M_2TeO_6$ (M = Ni, Co, Zn, Mg). *Chem. Mater.* **2011**, *23* (5), 1174–1181. https://doi.org/10.1021/cm102629g.

(19) Masese, T.; Yoshii, K.; Yamaguchi, Y.; Okumura, T.; Huang, Z. D.; Kato, M.; Kubota, K.; Furutani, J.; Orikasa, Y.; Senoh, H.; et al. Rechargeable Potassium-Ion Batteries with Honeycomb-Layered Tellurates as High Voltage Cathodes and Fast Potassium-Ion Conductors. *Nat. Commun.* **2018**, *9*, 3823. https://doi.org/10.1038/s41467-018-06343-6.

(20) Coelho, A. A.; Evans, J. S. O.; Lewis, J. W. Averaging the Intensity of Many-Layered Structures for Accurate Stacking-Fault Analysis Using Rietveld Refinement. *J. Appl. Crystallogr.* **2016**, *49* (5), 1740–1749. https://doi.org/10.1107/S1600576716013066.

(21) Carlier, D.; Blangero, M.; Ménétrier, M.; Pollet, M.; Doumerc, J.-P.; Delmas, C. Sodium Ion Mobility in Na_xCoO_2 ($0.6 < x < 0.75$) Cobaltites Studied by ^{23}Na MAS NMR. *Inorg. Chem.* **2009**, *48* (15), 7018–7025. https://doi.org/10.1021/ic900026c.

(22) Carlier, D.; Cheng, J. H.; Berthelot, R.; Guignard, M.; Yoncheva, M.; Stoyanova, R.; Hwang, B. J.; Delmas, C. The P2-$Na_{2/3}Co_{2/3}Mn_{1/3}O_2$ Phase: Structure, Physical Properties and Electrochemical Behavior as Positive Electrode in Sodium Battery. *Dalt. Trans.* **2011**, *40* (36), 9306–9312. https://doi.org/10.1039/C1DT10798D.

(23) Fauth, F.; Boer, R.; Gil-Ortiz, F.; Popescu, C.; Vallcorba, O.; Peral, I.; Fullà, D.; Benach, J.; Juanhuix, J. The Crystallography Stations at the Alba Synchrotron. *Eur. Phys. J. Plus* **2015**, *130* (8), 160. https://doi.org/10.1140/epjp/i2015-15160-y.

(24) Avdeev, M.; Hester, J. R. ECHIDNA: A Decade of High-Resolution Neutron Powder Diffraction at OPAL. *J. Appl. Crystallogr.* **2018**, *51* (6), 1597–1604. https://doi.org/10.1107/S1600576718014048.

TOC Graphic